Feeding-Related Traits Are Affected by Dosage of the *foraging* Gene in *Drosophila melanogaster*

Aaron M. Allen,[*,1] Ina Anreiter,[†,‡] Megan C. Neville,[§] and Marla B. Sokolowski[*,†,‡,2]

*Department of Cell and Systems Biology, University of Toronto, Ontario M5S 3G5, Canada, †Department of Ecology and Evolutionary Biology, University of Toronto, Ontario M5S 3B2, Canada, and ‡Child and Brain Development Program, Canadian Institute for Advanced Research (CIFAR), Toronto, Ontario M5G 1Z8, Canada, and §Centre for Neural Circuits and Behaviour, University of Oxford, OX1 3SR Oxford, UK

ORCID ID: 0000-0002-7462-8007 (M.B.S.)

ABSTRACT Nutrient acquisition and energy storage are critical parts of achieving metabolic homeostasis. The *foraging* gene in *Drosophila melanogaster* has previously been implicated in multiple feeding-related and metabolic traits. Before *foraging*'s functions can be further dissected, we need a precise genetic null mutant to definitively map its amorphic phenotypes. We used homologous recombination to precisely delete *foraging*, generating the *for⁰* null allele, and used recombineering to reintegrate a full copy of the gene, generating the *{for^{BAC}}* rescue allele. We show that a total loss of *foraging* expression in larvae results in reduced larval path length and food intake behavior, while conversely showing an increase in triglyceride levels. Furthermore, varying *foraging* gene dosage demonstrates a linear dose-response on these phenotypes in relation to *foraging* gene expression levels. These experiments have unequivocally proven a causal, dose-dependent relationship between the *foraging* gene and its pleiotropic influence on these feeding-related traits. Our analysis of *foraging*'s transcription start sites, termination sites, and splicing patterns using rapid amplification of cDNA ends (RACE) and full-length cDNA sequencing, revealed four independent promoters, *pr1–4*, that produce 21 transcripts with nine distinct open reading frames (ORFs). The use of alternative promoters and alternative splicing at the *foraging* locus creates diversity and flexibility in the regulation of gene expression, and ultimately function. Future studies will exploit these genetic tools to precisely dissect the isoform- and tissue-specific requirements of *foraging*'s functions and shed light on the genetic control of feeding-related traits involved in energy homeostasis.

KEYWORDS *foraging* gene; behavior; fat; larva; null mutant

FEEDING is critical to the development and survival of all organisms. During development, *Drosophila* larvae eat almost continuously. They experience rapid growth and deposit large amounts of triglycerides as energy stores. Once sufficient energy stores are reached, larvae stop feeding and alter their behavior to find pupariation sites (Edgar 2006). The size that a larva reaches and the level of stored nutrients has profound effects on survivorship, adult body size, and reproductive success (Bakker 1962). Consequently, the coor-

dination of larval movement, feeding, and energy storage is critical to the health of both the larva and adult. This coordination requires the communication of multiple tissue systems in *Drosophila* such as the brain, endocrine tissues, and fat body (Leopold and Perrimon 2007). As such, perturbations in a variety of tissue systems are sufficient to alter feeding behavior.

The *Drosophila melanogaster foraging* gene has become a classic model for the genetic influences on feeding-related behaviors (Sokolowski 2001). The differences in locomotion on a nutritive medium (path length) between the rover and sitter strains was mapped primarily to the *foraging* (*for*) gene, also known as *dg2*, which encodes a cGMP-dependent protein kinase (PKG) (de Belle *et al.* 1989; Kalderon and Rubin, 1989; Osborne *et al.* 1997). *foraging* is highly conserved at both the sequence and phenotypic levels (Manning *et al.* 2002; Fitzpatrick and Sokolowski 2004; Sokolowski 2010). The rover and sitter strains were subsequently shown

to differ in a suite of other behavioral and physiological traits, such as food intake and metabolism (Kaun *et al.* 2007; Kent *et al.* 2009), and as such *foraging* appears to be pleiotropic.

Much of the work conducted to date on the *foraging* gene relied on the rover and sitter *foraging* allelic variants (de Belle *et al.* 1989, 1993; Kaun *et al.* 2007, 2008). In rover and sitter strains, the entirety of their second chromosomes, where *foraging* resides, differ (Bauer and Sokolowski 1984; Sokolowski 1980). There is thus the potential for other loci to contribute to the phenotypic differences between these strains. To understand the contributions of the allelic variants of the *foraging* gene in these two strains, we need a precise understanding of the gene structure, its products, and its amorphic phenotypes. Since a genetic null allele of *foraging* would facilitate an examination of its potential pleiotropic effects on feeding-related behaviors in the larvae, we generated a precise deletion of the *foraging* gene by homologous recombination (HR; Gong and Golic 2003). To further examine the connection between genotype and phenotype we manipulated gene dosage using recombination-mediated genetic engineering (recombineering; Warming *et al.* 2005; Venken *et al.* 2006). Using these engineered allelic combinations, our analyses revealed an unequivocal role for *foraging* in larval movement, food intake, and energy storage. These experiments provide the solid foundation required for future research into determining tissue- and isoform-specific functions of *foraging*, as well as determining the causal differences between the rover and sitter allelic variants.

Materials and Methods

Fly strains and rearing

The rover and sitter strains have been in the lab for over 30 years and share a common first and third chromosome. They have been isogenized multiple times over the years, most recently between 2010 and 2012. The strains differ in their second pair of chromosomes where *foraging* resides. The path lengths of these rover and sitter strains are comparable to those collected from the field (Sokolowski 1980; Sokolowski *et al.* 1997) and the relative path length differences remain regardless of how the design of the path length assay has changed over the years (Anreiter *et al.* 2016). Fly strains for HR included $y^1 w^*$, *hsFLP*, *hsI-SceI/Y*, *hs-his* and $y^1 w^*$; *eyFLP5* and $y^1 w^*$, *eyFLP2*; *Pin/CyO*. The y^1, w^{67c23}, $P\{Crey\}1b$; sna^{Sco}/CyO strain (Siegal and Hartl 1996; BDSC #766) was used to resolve the *loxP* sequences to remove w^{+mC}, and delete *foraging*. The following *foraging* deletion strains were obtained from Bloomington Drosophila Stock Center: w^{1118}; *Df(2L)Exel7018/CyO* (Parks *et al.* 2004; BDSC #7789), $y^1 w^*$; *Df(2L)drm-P2*, *P{lacW}ND-PDSWk10101/SM6b* (Green *et al.* 2002; BDSC #6507), and w^{1118}; *Df(2L)ED243*, $P\{3'.RS5+3.3'\}ED243/SM6a$ (Ryder *et al.* 2004; Belay *et al.* 2007; BDSC #24122). The *foraging* for^0, for^{dup},

and *{for^{BAC}}* alleles were generated in this paper (see below); the for^0 mutants were maintained over a *CyO, act-GFP* balancer chromosome. Strains were reared in 40-ml vials with 10 ml of food and 170-ml bottles with 40 ml of food at $25 \pm 1°$ with a 12L:12D photoperiod with lights on at 0800 hr. The fly yeast–cornmeal–molasses–agar food recipe contained 1.5% sucrose, 1.4% agar, 3% glucose, 1.5% cornmeal, 1% wheat germ, 1% soy flour, 3% molasses, 3.5% yeast, 0.5% propionic acid, 0.2% Tegosept, and 1% ethanol in water. Mid third instar larvae were developmentally synchronized as described in Anreiter *et al.* (2016). Briefly, 5- to 7-day-old adults were allowed to oviposit on grape juice and agar media (45% grape juice, 2.5% ethanol, 2.5% acetic acid, 2% agar in water) for 20 hr. The following day, any hatched larvae were cleared from the media, followed by a 4-hr incubation; newly hatched larvae were seeded into a 100-mm diameter Petri dish containing 30 ml of food. The plates were incubated at $25 \pm 1°$ in a 12L:12D photoperiod with lights on at 0800 hr until they reached mid third instar (72 ± 2 hr post hatch).

Gene model characterization

All primer design, sequence analysis, chromatograph editing, contig assembly, *in-silico* cloning, and digestion confirmation was performed using the Geneious 8.1.7 software package (Kearse *et al.* 2012). All primer sequences are listed in Supplemental Material, Table S1. Transcription start sites (TSSs) were identified with 5′-rapid amplification of cDNA ends (RACE) experiments that used homopolymeric tailing (Michelson and Orkin 1982; Sambrook and Russell 2001) and RNA ligase using GeneRacer (Thermo Fisher Scientific, cat# L150202). Total RNA was extracted from pooled mid third instar larvae and adult flies from our rover and sitter strains with TriZOL Reagent (Thermo Fisher Scientific, cat# 15596018). RNA was reverse transcribed with Superscript III (Thermo Fisher Scientific, cat# 18080044) and primed with random hexamers and oligo dT primers. Terminal Transferase (New England Biolabs, Beverly, MA, cat# M0315S) was used to add a poly-guanosine tail to the 5′ end of the isolated cDNA. The 5′ ends of the transcripts were amplified with an oligo dC primer and gene-specific primer (comRT-R.3) targeting the coding sequence for the catalytic domain of the *foraging* gene. Transcription end sites (TESs) were identified by 3′-RACE using the GeneRacer Kit (ThermoFisher Scientific, cat# L150202) following the manufacturer's instructions, using a gene-specific primer (43S) targeting the catalytic domain. Splice variants were identified by RT-PCR using forward primers targeting the exons near the TSSs (TSS1-F, TSS2-F, TSS3-F, TSS4-F) and a reverse primer targeting the terminal exon (comORF3′-R). The resulting amplicons were cloned into the pGEM-Teasy vector (Promega, Madison, WI, cat# A1360). 144 RACE clones and 240 splice variant clones were then sequenced by Sanger sequencing on an ABI 3130xl Capillary Sequencer using BigDye Terminator v3.1 Cycle Sequencing Kit (Thermo Fisher Scientific, cat# 4337454).

Ends-out gene targeting

A 5-kb homology arm 5′ to the *foraging* gene was amplified with PCR using the primers HA1-F and HA1-R, with *Bsi*WI and *Asc*I sites, respectively. The 5′-homology arm was cloned into the *Bsi*WI and *Asc*I sites in the pW25 ends-out gene targeting vector (Gong and Golic 2004). An *attP* sequence (Thorpe and Smith 1998) was cloned into the *Kpn*I and *Not*I sites. The *attP* sequence was amplified with PCR (attP-F, attP-R) from the pCaryP vector (Groth *et al.* 2004) obtained from Addgene. A *Kpn*I was added to the forward primer and *Not*I and *Sbf*I sites were added to the reverse primer. A 5.2-kb homology arm 3′ to the *foraging* gene was amplified with PCR using primers HA2-F and HA2-R, and adding *Sbf*I and *Not*I sites to the forward and reverse primers, respectively. The 3′-homology arm was cloned into the *Sbf*I and *Not*I sites in the pW25-HA1-attP vector resulting in the the pW25$^{EO\text{-}for\text{-}attP}$ vector.

The pW25$^{EO\text{-}for\text{-}attP}$ vector was injected into a w^{1118} strain using *P* element transgenesis (performed by Genetic Services). This yielded an *X*-chromosome transformant. A series of crosses were conducted to mobilize the targeting construct and to allow HR (as in Demir and Dickson 2005). Briefly, ~ 1000 females containing the element were crossed into an *hs-Flp, hs-I-Sce*I-containing background, and embryos and L1 larvae were heat shocked at 38° for 2 hr on two consecutive days. Approximately 8000–10,000 progeny were then crossed into an *ey-Flp* background and were screened for red eye color. These crosses yielded eight integrations at the *foraging* locus; however, none of these had a deletion of the gene. The recombinants had integrated at either the 5′- or 3′-end of the locus, corresponding to the two homology arms. There are several reasons why this might have occurred, for one, *foraging* is a large gene and the size difference relative to the considerably smaller cloned construct might have impeded proper alignment. Alternatively, after sequencing the alleles where our construct had integrated (*for*^{HR1} and *for*^{HR4}), we found that the I-*Sce*I restriction sites remained uncut causing the cloned targeting construct to not linearize, which would have prevented spanning of the endogenous locus. This could have been due to inadequate heat shock, or a less than functional *hs-I-Sce*I transgene. Fortunately, it was still possible to generate a complete deletion of the *foraging* gene using the *loxP* sites in pW25, which were intended for removal of the w^{+mC} gene. To accomplish this, we crossed the 5′ and 3′ recombinants to make a *trans*-heterozygote in a *hs-Cre* background (BDSC #766). Embryos and L1 larvae were heat shocked at 38° for 2 hr on two consecutive days. Single male flies were then isolated and balanced. Twenty-four iso-male populations were established and screened for a deletion of the *foraging* locus. Four populations were identified as deletions, *for*^{0}, and eight as duplications, *for*^{dup}. The remainder showed no recombination.

Recombineering

The P[acman] vector was redesigned to be paired with the pW25-*attP* vector to have a minimal footprint upon reintegration of the engineered locus of interest. The BAC backbone was isolated by digesting the P[acman] cut with *Sal*I and *Sph*I. The w^{+mC} was isolated by digesting the P[acman] vector with *Eco*RI and *Sph*I. The *attB* sequence was amplified with PCR using the following primers, attB-F and attB-R. The attB-F primer included *Sal*I, *loxP*, *Asc*I, *Not*I, *Pac*I, and *Asi*SI sequences. The attB PCR product was cloned into the pSC-A-amp/kan (Agilent's Strataclone) and digested with *Sal*I and *Eco*RI. The purified P[acman], w^{+mC}, and the attB fragment were ligated together. This resulted in a vector with *loxP*, MCS, *attB*, w^{+mC} syntony. We called the resulting vector P[attlox]. The P[acman] clone CH321-64J02 BAC from Children's Hospital Oakland Research Institute (http://www.chori.org) was used as the source of the *foraging* gene sequence. A gap repair protocol (like Venken *et al.* 2006) was used to trim the larger BAC down to a 39.3-kb segment containing *foraging*. Left and right homology arms were amplified with PCR using the following primers: LA-F with an *Asc*I, LA-R with a *Not*I, RA-F with a *Not*I, and RA-R with an *Asi*SI. The left and right arms were cloned into the *Asc*I and *Asi*SI sites of the P[attlox] vector creating P[GAP]^{for}. P[GAP]^{for} was linearized with *Not*I and transformed into induced SW102 cells (Warming *et al.* 2005) containing the CH321-64J02 BAC. Recombination between the P[GAP]^{for} and the CH321-64J02 BAC yielded a *foraging*-specific BAC in the reengineered P[acman] vector, P[attlox]^{for}. As the BAC from the P[acman] library used here was generated using DNA isolated from the y^1;cn^1,bw^1,sp^1 strain, containing a naturally occurring *copia* transposable element in the *foraging* gene, we used *galK* selection (Warming *et al.* 2005) to remove the *copia* transposable element. A 579-bp left homology arm and a 580-bp right homology arm flanking the *copia* element were cloned into the *Xho*I/*Eco*RI and *Bam*HI/*Xba*I sites of the pGalK vector. The left arm was amplified with L-copia-F, and L-copia-R with an *Eco*RI site. The PCR product contained an internal *Xho*I site. The right arm was amplified with R-copia-F with a *Bam*HI site, and R-copia-R. The PCR product contained an internal *Xba*I site. The *Xho*I/*Xba*I LA-galK-RA fragment was transformed into SW102 cells containing the P[attlox]^{for} vector. The *for*-copia-galK BAC-containing cells were then transformed with a linear oligo, *for*-copia (Sigma Genesys). The resulting "wild-type" BAC was transformed into the EPI300 cells (Wild *et al.* 2002, acquired from Epicentre) and incorporated into the fly's genome using φC31 integration into the *attP2* landing site on the third-chromosomes (Groth *et al.* 2004). Transgenesis was done by Genetic Services.

Western blot analysis

Twenty mid third instar larvae (72 ± 2 hr post hatch) were homogenized on ice in 400 μl of lysis buffer (50 mM Tris-HCl pH 7.5, 10% glycerol, 150 mM NaCl, 1% Triton-X 100, 5 mM EDTA, 1× Halt Protease Inhibitor Cocktail (cat# 1862209)). Samples were centrifuged at 16,000 RCF at 4° and the supernatant was transferred to a new tube and placed on ice. Protein quantification was performed with Pierce BCA Protein Assay Kit (cat# 23227). Twenty micrograms of protein were denatured for 5 min at 100°. The samples were run on a 4%

stacking/7% resolving polyacrylamide and SDS gel at 150 V for 1 hr in running buffer (25 mM Tris-HCl, 200 mM glycine, 0.1% SDS). Proteins were transferred onto a nitrocellulose membrane (Pal, cat# 66485) at 100 V for 1 hr in transfer buffer (25 mM Tris-HCl, 200 mM glycine, 10% methanol). Blots were blocked for 2 hr in 5% nonfat milk in 0.1% Tween-20 in 1× TBS (0.1% TBST), and incubated with primary antibody for 1 hr, at a concentration of 1:10,000 for anti-FOR (Belay *et al.* 2007) and 1:5000 for anti-ACTIN (Sigma, St. Louis, MO). The blots were rinsed twice and washed 3× for 5 min with each rinse in 0.1% TBST. Blots were then incubated with HRP conjugated secondary (Jackson ImmunoResearch Laboratories; goat-anti-mouse-HRP cat# 115-035-146, goat-anti-guinea pig-HRP cat#106-035-003) at a concentration of 1:10,000 for 45 min. Finally, blots were rinsed twice and washed 3× as above, incubated for 5 min in General Electric Healthcare's Amersham ECL Prime Detection reagent (cat# RPN2232), exposed to X-ray film, and developed with Kodak developer and fixer.

Reverse transcription quantitative PCR

Total RNA was extracted from 72-hr-old larvae using the RNeasy Mini Kit (Qiagen Cat# 74104) and the corresponding RNase-free DNase set (QIAGEN, Valencia, CA, Cat# 79254), following the manufacturer's instructions for purification of total RNA from animal tissues. RNA was extracted from three biological replicates with $n = 20$ larvae per replicate. Following extraction RNA was quantified using a Nanodrop 2000c (Thermo Scientific), and RNA integrity was accessed by gel electrophoresis. Complementary DNA (cDNA) was synthesized with the iScript Advanced cDNA synthesis kit for RT-qPCR (Bio-Rad, Hercules, CA, Cat# 1725037), using 1 μg of RNA per sample, and following the manufacturer's instructions. RT-qPCR was performed on a CFX384 Touch Real-Time PCR Detection System (Bio-Rad), using SsoAdvanced Universal SYBR Green Supermix and gene-specific primers (Table S1). Primer efficiency was calculated and only primers with efficiencies between 99 and 105% were used (a-tub – 99.8%; act5C – 99%; for_com2–99.5%; for_pr1–100.08%; for_pr2–102.6%; for_pr3–101.8%; for_pr4–100.5%). Cycling conditions followed the manufacturer's protocol. Reference genes were initially selected based on stability values found in other studies (Ling and Salvaterra 2011; Ponton *et al.* 2011). Two reference genes were run (*α-Tub84B* and *Act5c*) and both had robust stability values (mean coefficient variance = 0.0296, mean *M* value = 0.0854). *α-Tub84B* had the lowest coefficient variance (0.0291) and was used to calculate relative expression values ($Eff_{(Target)}^{ACt}/Eff_{(Ref)}^{ACt}$) to determine differences between genotypes. Sample collection and data processing followed abbreviated MIQE recommendations (Taylor *et al.* 2010).

Path length

A detailed description of the foraging path length protocol is given in Anreiter *et al.* (2016). Briefly, foraging path length was measured using custom black rectangular Plexiglas plates (37 cm width, 60 cm length, 0.5 cm height) with 10 wells (0.5 mm depth, 9.5 cm diameter) arranged in a 2-by-5 pattern (Sokolowski *et al.* 1997). In the present study, mid third instar larvae (72 ± 2 hr post hatch) were randomly selected from the food plates and washed in a few drops of water. A homogenous yeast suspension (2:1 w/w) was spread across the wells creating a thin even layer in each well. Individual larvae were placed in the center of each well and covered with the lid of a 10-cm Petri dish. Larvae could move for 5 min after which the path length of each larva was traced onto the Petri dish lid. Path lengths were digitized using Fiji (Schindelin *et al.* 2012).

Food intake

We measured larval food intake using a new assay described here. Becton, Dickinson Falcon cell strainers (cat# 352350) were placed in 35-mm diameter Petri dishes and used to isolate and selectively feed groups of larvae. Fluorescent liquid food was prepared with 0.5% fluorescein (Sigma), 5% sucrose, and 5% yeast extraction New sentence. Third instar larvae (72 ± 2 hr post hatch) were removed from food plates, washed, and transferred in groups of 10 to cell strainers with 800 μl of liquid food. The above-mentioned Petri dish size and food volume resulted in the food being able to drain into the space below the mesh of the cell strainer, but remaining in contact with the mesh, flowing up by capillary action when it was eaten by the larvae. Once placed in the strainer, larvae were left to feed for 10 min, after which the strainers were lifted out of the food and rinsed with water, followed by three more washes with water. Washed individual larvae were placed into 0.2-ml wells of 96-well PCR plates and frozen at −20°. Frozen larvae were homogenized in 150 μl of 1× PBS with a 5/32″ stainless steel ball bearing (OPS Diagnostics) and agitation using a Qiagen Tissue Lyser. Samples were centrifuged at 3500 RCF for 15 min. Twenty microliters of the supernatant was then mixed with 180 μl of 1× PBS in a fluorimeter plate (Corning, cat# 3631) and excited at 488 nm. Emission was measured at 562 nm. Homogenates from larvae fed with food containing no fluorescein were used as controls.

Triglyceride analysis

Groups of 20 larvae (72 ± 2 hr post hatch) were homogenized in 1 ml of 0.1% Tween 20 in 1× PBS. Samples were incubated at 70° for 5 min, chilled on ice for 2 min, and used for triglyceride and total protein quantification. To measure triglyceride content, 20 μl of the above supernatant was mixed with 200 μl Infinity TAG Reagent (Thermo Scientific, cat# TR22421) in a 96-well spectrophotometer plate (Corning, cat# 351172). Samples were incubated at 37° for 10 min, and absorbance was measured at 540 nm. To quantify total protein levels for standardization of the triglyceride measures, 20 μl of the above supernatant was quantified for protein content using the Pierce BCA Protein Assay Kit (cat# 23227), following the manufacturer's instructions. BCA samples were incubated at 37° for 30 min, and absorbance was measured at 562 nm. Standard curves for triglycerides and albumin protein were used to calculate triglyceride and

protein concentration from the obtained absorbance values. Lipid levels are displayed as microgram glycerol per milligram protein.

Statistical analysis

Statistical analysis was performed in R (R Core Team 2013). The effects of genotype as well as blocking factors such as the date of the experiment were modeled with general linear models using the *lm* function, and *post hoc t*-tests were run to compute pairwise statistical significances. Multiple comparisons were corrected using the Holm method (Holm 1979). α of $P = 0.05$ was considered significant. Results of statistical analyses are provided in the figure captions. Graphs were plotted in R and edited in Inkscape.

Data availability

Strains are available upon request. Information in supplemental material: Table S1 contains primer names and sequences used in this study. Figure S1 describes the *for^{HR}* alleles, and the generation of the *for^0* null and *for^{dup}* alleles. Figure S2 shows verification of the *for^0* allele. Figure S3 shows construction and verification of the *for^{BAC}* construct. Figure S4 shows path length, food intake and fat levels of hemizygous rover and sitter larvae. Figure S5 shows *foraging* gene dosage and allelic contributions to *foraging* gene expression in whole larvae. Figure S6 provides *foraging* transcript sequences. File S1 provides the figure legends for Figures S1-S6.

Results

Characterizing the transcriptional complexity of the foraging gene

Previous studies have differed in the number and variety of *foraging* transcripts reported (Kalderon and Rubin 1989; Osborne *et al.* 1997; Stapleton *et al.* 2002). To produce an accurate model of the *foraging* gene, we first exhaustively identified the transcription start sites (TSSs) and transcription end sites (TESs) represented in mRNA transcripts produced by sequencing 144 RACE clones. We identified four separate TSSs and one TES, supporting a gene model for *foraging* that contains four independent minimal promoters (*pr1, pr2, pr3, pr4,* Figure 1) whose RNA products all splice into a common 3′-exon. A model containing multiple TSSs with one shared TES has also been shown for *foraging*'s orthologs in other organisms (Ørstavik *et al.* 1997; Stansberry *et al.* 2001). These promoters fall into two categories: *pr1, 2* and *4* are peaked, whereas *pr3* is broad. Peaked TSSs are typically found in regulated promoters, whereas broad TSSs are found in constitutive promoters (Hoskins *et al.* 2011). All four promoters contain clear consensus core promoter Initiator (Inr) and Downstream Promoter Elements.

We next surveyed the alternative splicing complexity found in *foraging* mRNA. We isolated and sequenced 240 full-length cDNA clones which represented 21 distinct mRNA transcripts, encoding nine distinct open reading frames (ORFs; Figure 1). Due to the shared 3′-end of the transcripts, these variants differ in their 5′-UTR and the corresponding N-terminal coding sequences of their ORFs. The coding sequences for the cGMP-binding domains as well as the kinase domain of the protein products were all located in the shared exons. Ten of the 21 transcripts are currently annotated in Flybase (Attrill *et al.* 2016) making 11 transcripts novel. Six of these 11 transcripts exhibit a novel instance of exon skipping in the *foraging* gene (RL, RM, RN, RO, RP, RS), all of which reduce N-terminal coding sequence. Although these results suggest a more complex gene structure compared to previous reports, all the new variants identified here include the same originally described 12 exons (Kalderon and Rubin 1989).

Generation of a novel and precise foraging null allele (for^0)

To generate a null mutation of the *foraging* gene we used the ends-out gene targeting system (Gong and Golic 2004). Regions of homology on either side of the *foraging* gene (Figure 2A) were cloned into the pW25 vector. The intended recombination event would delete all of *foraging*, leaving a *loxP* and *attP* site (Figure 2B). Mobilization of this targeting construct yielded eight second chromosome integrations, none of which deleted the *foraging* locus as expected. However, we did find separate integration events at both the 5′- and 3′-end of the locus (Figure S1). These recombination events allowed us to generate the intended null mutation of *foraging* (Figure 2B) by using the *loxP* site-specific recombination sequences in the pW25 vector, which were intended for removal of the *white^{+mC}* gene used to identify integration events (Figure S1). To accomplish this, we induced a recombination event resulting in the deletion of the entire locus by crossing the 5′-*loxP* element (integrant *for^{HR4}*) to the 3′-*loxP* element (integrant *for^{HR1}*), generating a *trans*-heterozygous mutant in the presence of a *Cre* recombinase. This approach successfully generated a null allele of *foraging*, which we called *for^0*, and a duplication allele, which we called *for^{dup}*. PCR, Southern blotting, sequencing, and restriction enzyme analysis (Figure S2 and data not shown) confirmed that the *Cre* recombinants were indeed deletions of the *foraging* locus. Critically, RT-PCR and western blot experiments of homozygous *for^0* larvae did not detect any RNA or protein (Figure 2, D and E). Thus, our newly generated *for^0* mutant is a true null allele of the *foraging* gene.

Generation and genomic integration of a foraging BAC

To manipulate *foraging* gene dosage, we used recombineering to generate a novel transgenic copy of the entire *foraging* locus that we named {*for^{BAC}*}. The P[acman] library was used as a source of our {*for^{BAC}*} allele (Venken *et al.* 2006). This BAC library was generated from the *y^1;cn^1,bw^1,sp^1* strain that contained a *copia* transposable element within the *foraging* gene. Extensive DNA sequencing has shown that this *copia* element does not occur in any of our laboratory strains, nor have we detected it in any allele of the *foraging* gene other
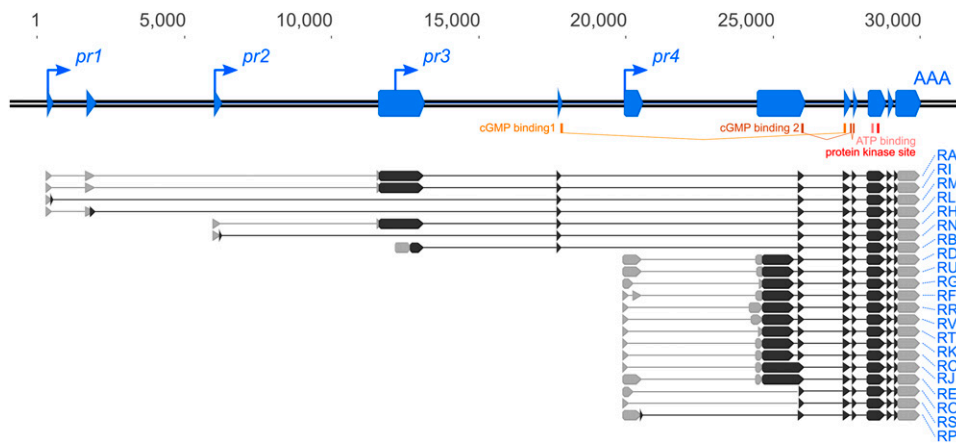
Figure 1 Schematic of the *foraging* gene and associated features. The *D. melanogaster foraging* gene has four promoters that produce 21 transcripts and nine open reading frames (ORFs). The transcription start sites (*pr1–4*, up-and-right arrows) and transcription end site (AAA) were identified with rapid amplification of cDNA ends (RACE). The splicing patterns of the transcripts were identified by sequencing full-length cDNAs. Exons (blue boxes) are annotated along the locus (double black line) with the transcripts below. UTRs (gray boxes), ORFs (black boxes), cGMP-binding domains (yellow), ATP-binding domain (pink), and kinase domains (red) are also annotated. RA through RK were previously annotated on FlyBase.

than the reference genome line (data not shown). We successfully removed this *copia* element using the *galK*-selection method (Warming *et al.* 2005; Figure S3). Furthermore, the gap repair method (Venken *et al.* 2006) we used here yielded a BAC spanning the 35-kb *foraging* locus, removing the rest of the large genomic region included in BAC CHORI-64J02 (Figure S3). The resulting P[attlox]^{for} construct (Figure S3) was successfully incorporated into the fly's genome using φC31 integrase into the *attP2* landing site (Groth *et al.* 2004), generating the *{for^{BAC}}* allele (Figure 2C). RT-PCR and western blot analyses of the *{for^{BAC}}* allele showed similar expression patterns to the wild-type sitter strain (Figure 2, D and E).

foraging BAC rescue of for^0 pupal lethality

The generation of a *for^0* allele allowed us to determine whether *foraging* is an essential gene. We found that homozygous *for^0* larvae died in the late pupal (pharate adult) stage. The recessive pupal lethality of homozygous *for^0* flies was fully rescued by a single copy of the *{for^{BAC}}* allele, indicating that the 35-kb genomic fragment of the *foraging* gene in the BAC contained sufficient regulatory elements to fully restore the lethality of *foraging* null to wild-type; all adults were viable and fertile (data not shown). The survivorship of the *for^0* null mutants from first larval instar into the pupal stage was comparable to that of wild-type animals. The fact that late pharate homozygous *for^0* animals dissected from their pupal cases did not survive (data not shown) suggested that the lethality did not result from an inability to eclose from their pupal cases. Several previously published genomic deletions spanning all or part of the *foraging* gene were unable to complement the pupal lethality of the *for^0* mutant. We tested the *Df(2L)Exel7018* (Parks *et al.* 2004), *Df(2L)drm^{P2}* (Green *et al.* 2002), and *Df(2L)ED243* (Ryder *et al.* 2004) deletions, all of which failed to complement the *for^0* allele (data not shown). Like the *for^0* homozygous null,

all three heterozygous combinations of these deletions with *for^0* were pharate adult lethal.

foraging gene dosage and allelic contributions significantly affect larval foraging path length

Metabolic homeostasis requires a balance of energy expenditure, energy acquisition, and energy storage. Food search and navigation of a nutritional environment is vital to this process. We first examined the larval path length phenotypes of the newly generated strains that differed in the dosage of the *foraging* gene. As mentioned previously, the recombination event that generated the *for^0* null allele also generated an allele with a duplication of the *foraging* gene locus, *for^{dup}* (Figure S1). Larvae homozygous for the *for^{dup}* allele showed longer path lengths than larvae with homozygous *for^0* null alleles (Figure 3A). We next examined the larval path length for the null (*for^0*), rescue (*for^0;{for^{BAC}}*), and over expresser (*for^s;{for^{BAC}}*). The insertion of a *{for^{BAC}}* into the *for^0* genetic background, which we call our rescue strain (*for^0; {for^{BAC}}*), significantly increased mean larval path lengths on yeast (Figure 3A). Furthermore, insertion of a *{for^{BAC}}* into the *for^s* genetic background (*for^s;{for^{BAC}}*) increased mean larval path lengths significantly more, relative to both *for^0;{for^{BAC}}* and *for^0*. These results showed that increasing *foraging* gene expression by increasing gene dosage resulted in an increase in larval path length on yeast. We then investigated the allelic relationships between the wild-type rover (*for^R*) and sitter (*for^s*) alleles on larval path lengths, and asked if our gene dosage experiments can inform on the nature of rovers and sitters. As previously shown (Sokolowski 1980; de Belle *et al.* 1989; Osborne *et al.* 1997; Kaun *et al.* 2007), rover larvae had longer mean path lengths on yeast than sitters, and rover/sitter heterozygotes were indistinguishable from rover homozygotes (Figure 3C) confirming the dominance of the rover allele over the sitter allele. The rover/sitter difference in path
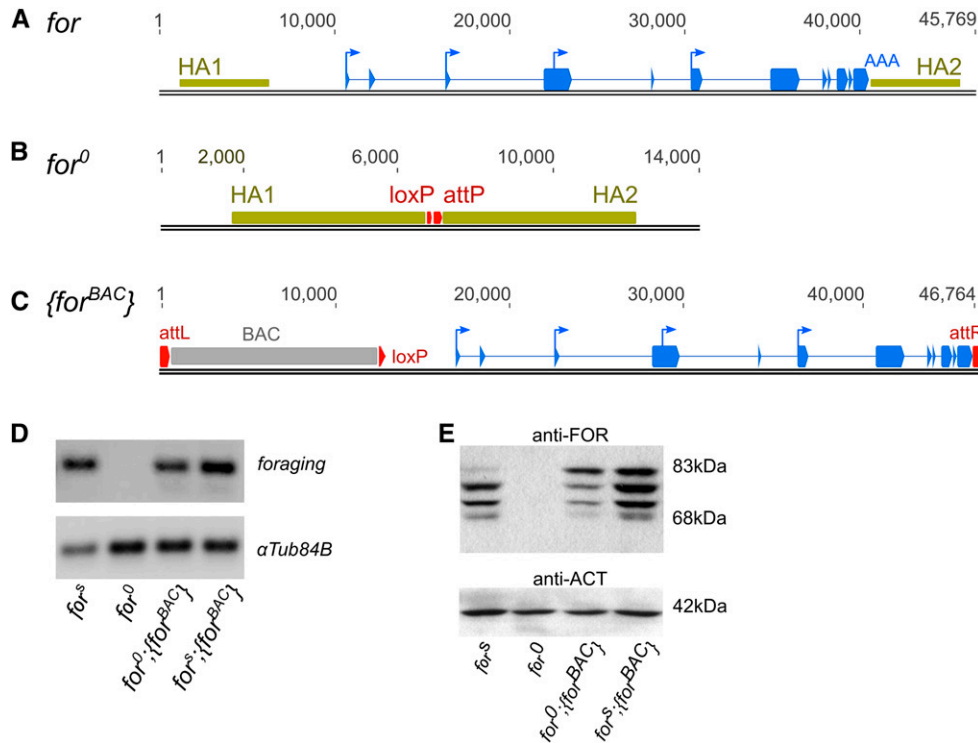
Figure 2 Generation of for^0 and $\{for^{BAC}\}$ alleles. (A) Schematic of the *D. melanogaster foraging* locus with 5-kb homology arms (HA1, HA2, tan boxes) that were cloned into the pW25-attP vector. (B) Schematic of the for^0 allele following recombination. The *foraging* gene was replaced with a *loxP* and *attP* site. (C) Schematic of the $\{for^{BAC}\}$ allele following ϕC31 integration at the *attP2* site. (D) RT-PCR of whole larval homogenates of homozygous for^s, for^0, for^0; $\{for^{BAC}\}$, and for^s; $\{for^{BAC}\}$ allelic combinations. Primers common to all annotated *foraging* transcripts, com2-F and com2-R, were used to amplify *foraging*. (E) Western blot of whole larval homogenates of homozygous for^s, for^0, for^0; $\{for^{BAC}\}$, and for^s; $\{for^{BAC}\}$ individuals. Size markings are listed to the right of the blots, and antibodies are listed above each blot.

length was maintained when the alleles were hemizygous with the for^0 allele (Figure S4A).

foraging gene dosage and allelic contributions significantly affect larval food intake

Once a larva has found a food source, it needs to ingest the food to acquire the nutrients needed for metamorphosis. Feeding rate can affect body size, which in turn can affect survival. We moved on to measure food intake, the next step in energy acquisition. We developed a novel fluorescence-based food intake assay. By using a liquid food medium and cell strainer dishes, larvae can be rapidly assayed and cleaned and frozen prior to quantification with a fluorometer. *foraging* null larvae (for^0) had lower food intake than duplication allele (for^{dup}) larvae (Figure 4A). The null allele also had lower mean food intake compared to the rescue (for^0; $\{for^{BAC}\}$) and over expresser (for^s; $\{for^{BAC}\}$) larvae (Figure 4B). Therefore, increasing *foraging* gene copy number increased food intake in a dose-dependent manner like that seen for the mean larval path length on yeast (Figure 3 and Figure 4). As with path length, we examined rovers and sitters for food intake in the light of the gene dosage experiments. Consistent with previous work that used a different food intake assay (Kaun *et al.* 2007, 2008), we found that rovers had lower food intake than sitters (Figure 4C). Previously, rover/sitter heterozygotes had not been tested for food intake. Interestingly, the food intake of rover/sitter heterozygotes was indistinguishable from that of homozygous sitter larvae (Figure 4C). This is the opposite pattern seen in our path length results. This rover/sitter difference was also seen

when the alleles were hemizygous with the for^0 allele (Figure S4B). This suggested that the pattern of dominance for food intake differed from that for larval path length, with the sitter allele being dominant to the rover allele for food intake.

Increased foraging gene dosage significantly decreases triglyceride levels

Fat stores are critical for survival during metamorphosis. After feeding, the acquired nutrients need to be digested and absorbed. Absorbed nutrients are primarily stored as triglycerides in the fat body of the larva. With our results showing that *foraging* plays a role in both energy expenditure and intake measures, we then moved on to measure fat levels, a component of energy storage. We used our *foraging* dosage-specific allelic series to analyze lipid storage. Whole larval homogenates were incubated with the Infinity TAG Reagent (Thermo Scientific), which contains a lipase, dissociating fatty acids from the glycerol backbone of triglycerides (as well as monoglycerides and diglycerides). Free glycerol is then colorimetrically quantified with a spectrophotometer. The for^0 null larvae had higher triglyceride levels than the for^{dup} duplication larvae (Figure 5A). Similarly, the for^0 null mutants had significantly higher mean triglycerides than the rescue (for^0; $\{for^{BAC}\}$) and the over expresser (for^s; $\{for^{BAC}\}$) strains (Figure 5B), suggesting that increased *foraging* gene dosage decreased triglyceride levels. We then assayed rovers and sitters to see if they differed in triglyceride levels, and to see what their phenotype implies about their relative expression considering the gene dosage. We found that rovers had lower mean triglyceride levels than sitters and that
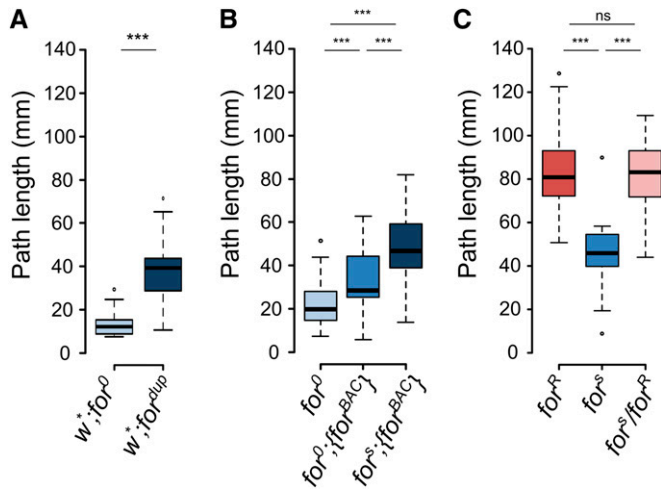
Figure 3 *foraging* gene dosage and allelic contributions to larval path length. (A) Larval path length of homozygous *for⁰* and *for^dup* individuals. Increasing gene copy number increases path length ($t = -8.24$, df = 34.31, $P = 1.2e-9$). (B) Path length on yeast of homozygous *for⁰*, *for⁰;{for^BAC}*, and *for^s;{for^BAC}* individuals. Increasing gene copy number increases path length ($F_{(2,105)} = 32.3$, $P = 1.2e-11$). (C) Larval path length behavior of homozygous *for^R*, *for^s* and heterozygous *for^R/for^s* individuals ($F_{(2,87)} = 46.4$, $P = 1.9e-14$). mm, millimeters; ns, nonsignificant; *** $P < 0.001$.

Figure 4 *foraging* gene dosage and allelic contributions to larval food intake. (A) Larval food intake of homozygous *for⁰* and *for^dup* individuals. Increasing gene copy number increases food intake ($t = -2.65$, df = 29.08, $P = 0.012$). (B) Food intake of homozygous *for⁰*, *for⁰;{for^BAC}*, and *for^s;{for^BAC}* individuals. Increasing gene copy number increases food intake ($F_{(2,249)} = 70.4$, $P < 2.2e-16$). (C) Larval food intake of homozygous *for^R*, *for^s* and heterozygous *for^R/for^s* individuals ($F_{(2,213)} = 10.0$, $P = 7.1e-5$). a.u., arbitrary fluorescence units; ns, nonsignificant; * $P < 0.05$, *** $P < 0.001$.

rover/sitter heterozygotes had an intermediate level of mean triglycerides (Figure 5C). This rover/sitter difference was maintained when the alleles were hemizygous with the *for⁰* allele (Figure S4C).

foraging gene dosage and allelic contributions to foraging gene expression

We next set out to verify that our allelic combinations of *foraging* used to manipulate gene dosage do indeed confer differences in gene expression. We used reverse transcription quantitative PCR (RT-qPCR) to characterize the expression levels of the *foraging* gene in whole larval homogenates. We probed the common coding region of the gene to capture all known transcripts, as well as the four promoter regions (Figure 1 and Figure 6A). We identified clear differences in expression between our homozygous *foraging* null (*for⁰*), our homozygous genomic rescue (*for⁰;{for^BAC}*), and homozygous over expresser (*for^s;{for^BAC}*) larvae for all regions assayed (Figure 6, B–F). As expected *for⁰* showed no expression, *for⁰;{for^BAC}* showed significantly higher expression than the null, and *for^s;{for^BAC}* showed significantly higher expression than both the null and the rescue. We saw no difference between homozygous rovers, sitters, and rover/sitter heterozygotes, but hemizygous rovers and sitters (*for^R/for⁰* and *for^s/for⁰*) had half the expression of *foraging* (Figure S5). Osborne *et al.* (1997) showed using northern analyses that the *foraging* mRNA levels in whole adult rovers were higher than in sitters. In contrast, in the present study using RT-qPCR we assayed *foraging* mRNA levels from 72-hr post hatch whole larvae and found no differences in expression between rovers and sitters. The effects of the different allelic
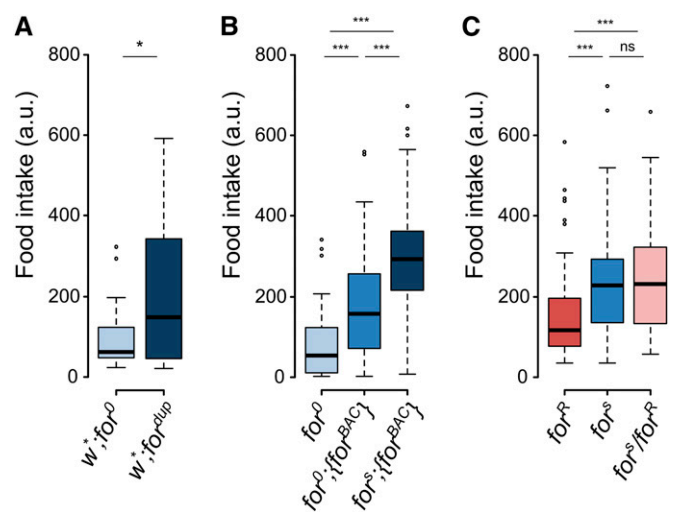
combinations were similar across the different promoters and were consistent with the pattern seen for the common coding region. The only exception to this pattern was the expression of *pr1*, which had lower expression in the *{for^BAC}* allele relative to the *for^s* allele, suggesting that the expression pattern of our rescue line differs in *pr1* expression compared to wild type (Figure 6B). There were, however, large differences in the level of expression between the different promoters. Notably, *pr1* and *pr3* made up most of the *foraging* expression (Figure 6, B and D, respectively). Conversely, *pr2* and *pr4* only represent a small fraction of the total *foraging* expression (Figure 6, C and D, respectively). The signal seen with the *pr3* primer set also captured some of the isoforms produced from *pr1* and *pr2* since the transcript RB has no unique element and is nested within RA, RH, and RI. These data would suggest that in the whole larva, *pr1* and *pr3* contribute roughly equally to the overall expression levels seen from *foraging* and they represent most of the expression, with *pr2* and *pr4* having overall low expression levels, or are expressed in only a small subset of *foraging*-expressing cells.

Modeling the effect of foraging gene dosage on path length, food intake, and triglyceride phenotypes

We then modeled the continuous effect of gene copy number on the path length, food intake, fat levels, and gene expression phenotypes. We performed linear regressions on the data (Figure 3B, Figure 4B, Figure 5B, and Figure 6F), but with the genotype variable exchanged for gene dosage number (null = 0, rescue = 2, over = 4). The phenotypes were normalized to rescue strain and are plotted as a percent. From
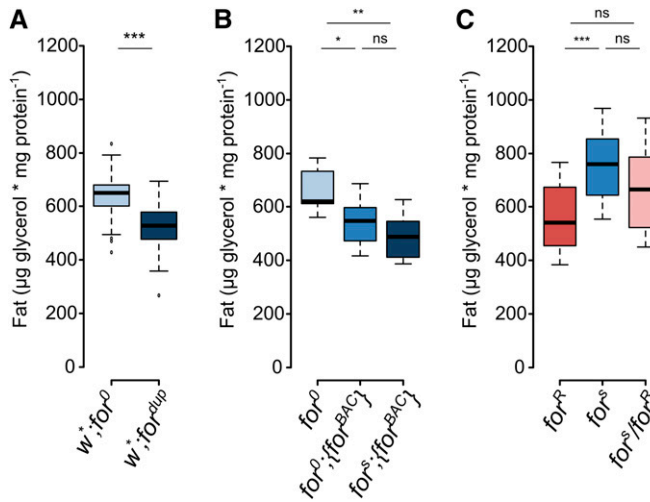
Figure 5 *foraging* gene dosage and allelic contributions to larval fat levels. (A) Larval triglyceride levels of homozygous *for[0]* and *for[dup]* individuals. Increasing gene copy number decreases fat levels ($t = 91.03$, df = 1, $P = 4.4e-9$). (B) triglyceride levels of homozygous *for[0]*, *for[0];{for[BAC]}*, and *for[s];{for[BAC]}*. Increasing gene copy number decreases triglyceride levels ($F_{(2,21)} = 8.4$, $P = 0.002$). (C) Larval triglyceride levels of homozygous *for[R]*, *for[s]* and heterozygous *for[R]/for[s]* individuals ($F_{(2,45)} = 8.36$, $P = 0.00082$). *** $P < 0.001$, ** $P < 0.01$, * $P < 0.05$; ns, nonsignificant.

these regression lines (solid lines) and their 95% confidence intervals (faded boxes), we can clearly see the linear gene dosage effect of the *foraging* gene on the phenotypes of path length, food intake, and triglyceride levels (Figure 7, A–C). The effect of gene dosage on *foraging* gene expression is added for comparison (Figure 7D). The regressions were highly significant, and had R^2 values of between 0.3 and 0.4 for path length, food intake, and fat, but naturally much higher for gene expression, $R^2 = 0.98$ (Figure 7, A–D). Aside from gene expression, food intake had the steepest slope and fat levels had the shallowest (Figure 7E). Therefore, increasing *foraging* gene expression had a larger relative effect on food intake than it did on path length (food intake *vs.* path length, $t_{(320)} = 3.21$, $P = 1.46e-3$) or fat levels (food intake *vs.* fat, $t_{(280)} = 11.8$, $P = 1.99e-26$).

Discussion

Meeting energy requirements and maintaining energy homeostasis is critical for every organism. The coordination of food searching, food acquisition, and nutrient storage is necessary for meeting the challenges of changing environments. Selecting for one of these traits has been shown to have knock-on effects on the others (Sewell *et al.* 1974; Burnet *et al.* 1977; Joshi and Mueller 1988; Sokolowski *et al.* 1997). The extensive behavioral literature on the *foraging* gene serves as an important example of how allelic variants can be used to infer the functions of a gene. Much of the work conducted to date on the *foraging* gene relied on the rover and sitter allelic variants (de Belle *et al.* 1989, 1993; Kaun *et al.* 2007) and studies using cDNA constructs driving expression beyond wild-type levels (Osborne *et al.* 1997; Mery

et al. 2007; Kaun *et al.* 2008; Burns *et al.* 2012). However, it is important to note that this approach may only uncover a subset of *foraging*'s functions and does not allow for a genetic dissection of the relationship between them.

As a first step toward a comprehensive characterization of the *foraging* gene, we carried out an exhaustive molecular analysis, defining the transcriptional complexity of *foraging* expression in larvae. We have defined four independent promoters, producing 21 mRNA transcripts between them, 11 of which are novel. This complexity lends support to the idea that *foraging*'s gene products might be differentially regulated to produce its multiple phenotypes. All *foraging* transcripts encode ORFs with a common cGMP-binding and kinase domain; however, isoforms notably differ in their N-termini. Furthermore, among the novel transcripts, there is a class that exhibits exon skipping, relative to the other transcripts produced from the same promoter. This exon skipping results in a roughly 300–500 (depending on the transcript) amino acid truncation at the N-termini, which includes both the autoinhibitory domain and dimerization domain. Interestingly, the N-termini of PKGs are critical in determining PKG-substrate interaction (Pearce *et al.* 2010). So, *foraging*'s function not only depends on which cell a promoter drives expression, but also what substrate *foraging*'s proteins can bind.

A precise genetic null allele allows us to conclusively associate *foraging*'s phenotypes, and lay the foundation for future genetic dissection of *foraging*'s isoform- and tissue-specific functions. In the present study, we precisely deleted the entire 35-kb *foraging* gene using HR to generate a *for[0]* null mutant, and we generated a transgenic *{for[BAC]}* allele using recombineering. We could study the resulting loss-of-function phenotypes in *D. melanogaster* larvae despite the pupal lethality of the homozygous *for[0]* null mutant. We have shown that *foraging* plays a critical role in each of the feeding-related phenotypes studied here. Increasing *foraging* gene copy number, both by insertion of the *{for[BAC]}* allele in a wild-type background, as well as the duplication at the locus itself, increased both larval path length on yeast and food intake while reducing triglyceride levels.

We have provided compelling evidence for a causal relationship between the *foraging* gene and its three larval phenotypes, using gene dosage. The null mutant generated here also provides a basis for conditional rescue using transcript-specific cDNA lines, and tissue-specific *GAL4* drivers. These tools will allow the rescue of the amorphic phenotype with spatial- and temporal-specific expression using the various *foraging* isoforms. Mapping the promoters and their transcripts involved in foraging-related phenotypes will allow us to narrow down DNA sequences in the locus that contain putative regulatory elements. This will in turn make it possible to select candidate SNPs between rovers and sitters that might be driving differences seen in expression and behavior. The fact that our *{for[BAC]}* construct rescues the null phenotypes, suggests that the 35-kb locus of the *foraging* gene contains the required regulatory elements to drive the expression
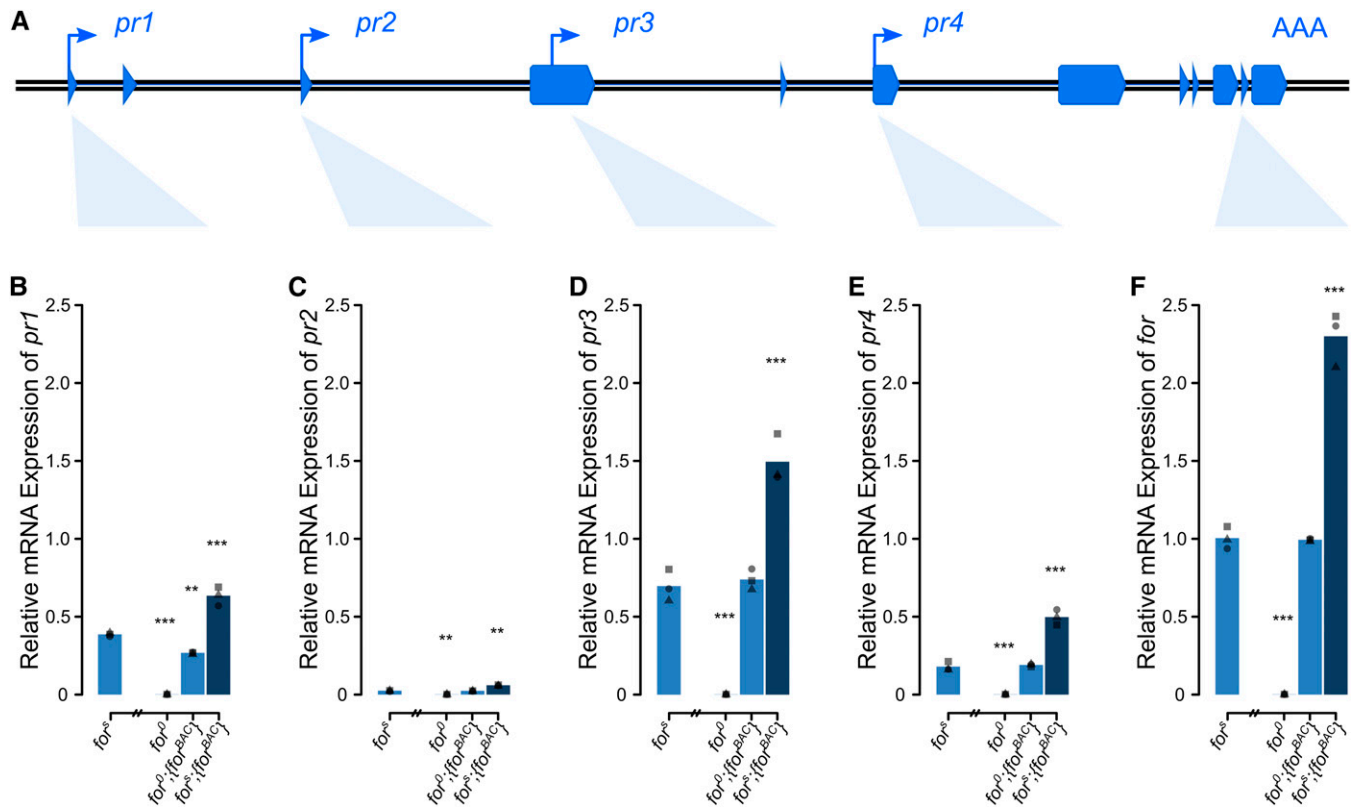
Figure 6 *foraging* gene dosage and allelic contributions to *foraging* gene expression in whole larvae. Expression of *foraging* mRNA of homozygous *for⁰*, *for⁰;{forᴮᴬᶜ}*, *forˢ;{forᴮᴬᶜ}*, and *forˢ* whole larvae homogenates amplifying each promoter region and the common coding region. (A) Schematic of the *foraging* (as in Figure 1). Promoter-specific regions targeted for qPCR identified by the upper vertex of the light blue triangles. (B) *pr1*-specific ($F_{(3,8)}$ =218.4, P = 5.2e−8), (C) *pr2*-specific ($F_{(3,8)}$ = 360.2, P = 7.2e−9), (D) *pr* ($F_{(3,8)}$ = 113.6, P = 6.7e−7), (E) *pr4*-specific ($F_{(3,8)}$ = 152.6, P = 2.1e−7), and (F) common coding ($F_{(3,8)}$ = 301.6, P = 1.4e−8) expression of regions of *foraging* quantified RT-qPCR. Due to the gene structure, *pr3* is not specific and amplifies a subset of *pr1* and *pr2*, as well. (B–F) Individual data points are plotted (n = 3/genotype; triangle, square, circle) with a bar representing the mean of the three samples. All the ΔΔCts were calculated relative to the mean *forˢ* ΔCt for the common coding region in F. *** $P < 0.001$, ** $P < 0.01$; *P*-values are relative to *forˢ*.

necessary for viability, path length, food intake, and triglyceride levels. We have sequenced the *foraging* gene of rovers and sitters and found that there are >300 SNPs that differ between these lines. The vast majority of these differences lie in the noncoding region of the gene, suggesting key allelic differences are likely associated with the regulation of gene expression rather than the modification of the function of the kinase itself. Nevertheless, this number of SNPs is far too extensive to address each SNP as a candidate causal SNP. Thus, narrowing down putative regulatory regions will be the first step to address the underlying DNA differences that drive rover and sitter behavior.

We quantified the expression of the individual promoters of *foraging* in whole larvae and saw striking differences in expression levels. These different expression levels show that the isoforms of *foraging* are differentially regulated. This differential regulation may result in different isoforms being expressed in different tissues at different times, and at different levels. Microarray data from Fly Atlas and RNA-Seq data from modENCODE support this possibility. *foraging* is expressed in many tissues (Chintapalli *et al.* 2007) throughout development (Graveley *et al.* 2011). Furthermore, isoform-specific exons are

differentially expressed in different tissues (Brown *et al.* 2014). *foraging*'s function may be tissue-specific or distributed across many tissue systems for any given phenotype. *foraging*'s tissue-specific requirements for the larval phenotypes studied here are currently not known.

Whether *foraging*'s role in these phenotypes is due to acute or developmental functions of its gene products is also unknown. Formation of the proper circuits for feeding behavior are developmentally regulated (Friedrich *et al.* 2016), and *foraging* mutants have been shown to alter nervous system development in the embryo (Peng *et al.* 2016). It is possible that a portion of *foraging*'s function in the larva may be due to such a role in embryo development. Alternatively, *foraging* may be functioning acutely during the behavior to elicit its phenotypic effects. *hugin* neurons, or their targets, are candidate cells for *foraging* function since acute manipulation of these cells can alter larval locomotion and feeding (Schoofs *et al.* 2014). A lack of *foraging* in *D. melanogaster* could also affect larval path length or feeding due to altered muscle function, making the muscles less sensitive to incoming neuronal stimuli. *foraging*'s ortholog in mammals has been characterized for its role in muscle function (Pfeifer *et al.* 1998;
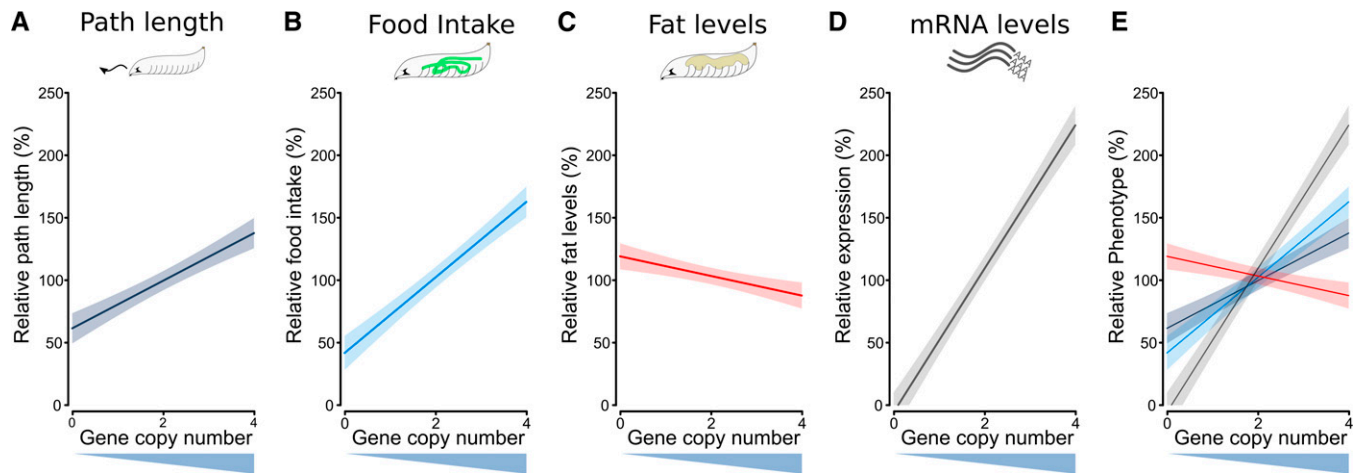
Figure 7 Modeled effects of *foraging* gene dosage on relative path length, food intake, fat, and expression. The fitted responses (solid lines) are plotted with 95% confidence intervals (greyed boxes). Raw data from Figure 3B, Figure 4B, Figure 5B, and Figure 6F were normalized to the mean of *for^s;{for^{BAC}}* for each phenotype; (A) path length (R^2 = 0.374, slope = 19.05, intercept = 61.90, $F_{(1,106)}$ = 64.81, P = 1.3e−12), (B) food intake (R^2 = 0.358, slope = 30.23, intercept = 42.17, $F_{(1,250)}$ = 141.0, P < 2.2e−16), (C) fat levels (R^2 = 0.399, slope = −7.850, intercept = 119.5, $F_{(1,22)}$ = 16.29, P = 5.5e−4), (D) mRNA expression (R^2 = 0.984, slope = 57.41, intercept = −5.227, $F_{(1,7)}$ =502.5, P = 8.9e−8). (E) path length, food intake, fat levels, and gene expression overlaid on each other for comparison.

Weber *et al.* 2007). As for the triglyceride level phenotype, *foraging* is highly expressed in the fat body of the larva (Chintipalli *et al.* 2007; Brown *et al.* 2014), and may function locally in the fat body to alter triglyceride levels. *foraging*'s orthologs have previously been shown to affect fat levels (Raizen *et al.* 2006; Miyashita *et al.* 2009). Future studies will unravel *foraging*'s tissue-specific requirements for larval path length, food intake, and triglyceride levels.

The use of a kinase such as *foraging* that can regulate the activity of many targets might allow the coregulation of physiologically related phenotypes such as path length, food intake, and fat in response to external inputs or internal physiological state. This would be important since behavioral responses are complex, originating from the interaction of different cellular processes in different tissues (*e.g.*, changes in movement on food might be brought on by an interaction of fat metabolism, nervous system, and muscle activation), and need to be coordinated. Without knowing the precise tissues or cells where *foraging* expression is required to alter its associated behaviors, it is difficult to speculate on the nature of the gene networks in which it resides. That being said, previous genetic evidence has suggested possible interaction with *insulin*-signaling and *foxo*-signaling (Kent *et al.* 2009; Kanao *et al.* 2012).

foraging has been implicated in a variety of adult phenotypes (Sokolowski 2010). Given the pupal lethality seen in the *foraging* null mutant, it is possible that some of the previously associated adult phenotypes may be developmental in origin, possibly resulting from differential neurogenesis. In the present study, the pupal lethality of the *foraging* null restricted its use to larval rather than adult phenotypes. We have recently, however, overcome this limitation by using temperature-sensitive *foraging* RNAi conditional-knockdown, specifically during adulthood (data not shown). These results

along with the results of the present study show that *foraging* is not required for viability specifically in the larval and adult stages, but is required for viability during pupal development.

In the present study, we described and characterized the structure of the *foraging* gene. We generated a *foraging* null mutant, *for^0*, using HR. This mutant was pupal lethal, showing that *foraging* gene products are not required for viability during larval development. This allowed us to evaluate the feeding-related behavior and metabolic state of the *for^0* null larvae. We have shown that *foraging* influences how larvae navigate their food environment, how they ingest nutrients, and further deposits those nutrients into fat. Our deletion study combined with the genomic rescue experiments have unequivocally proven a causal, dose-dependent relationship between the *foraging* gene and its pleiotropic influence on these feeding-related traits. Future studies will shed further light onto *foraging*'s regulation and the nature of the rover and sitter alleles.

Literature Cited

Anreiter, I., O. E. Vasquez, A. M. Allen, and M. B. Sokolowski, 2016 Foraging path-length protocol for Drosophila melanogaster larvae. J. Vis. Exp. DOI: 10.3791/53980.

Attrill, H., K. Falls, J. L. Goodman, G. H. Millburn, G. Antonazzo *et al.* 2016 FlyBase: establishing a gene group resource for Drosophila melanogaster. Nucleic Acids Res. 44: D786–D792.

Bakker, K., 1962 An analysis of factors which determine success in competition for food among larvae of Drosophila melanogaster. Arch. Néerl. Zool. 14: 200–281.

Bauer, S. J., and M. B. Sokolowski, 1984 Larval foraging behavior in isofemale lines of Drosophila melanogaster and D. pseudoobscura. J. Hered. 75: 131–134.

Belay, A. T., R. Scheiner, A. K.-C. So, S. J. Douglas, M. Chakaborty-Chatterjee *et al.*, 2007 The foraging gene of Drosophila melanogaster: spatial-expression analysis and sucrose responsiveness. J. Comp. Neurol. 504: 570–582.

Brown, J. B., N. Boley, R. Eisman, G. E. May, M. H. Stoiber *et al.*, 2014 Diversity and dynamics of the Drosophila transcriptome. Nature 512: 393–399.

Burnet, B., D. Sewell, M. Bos, K. Bakker, L. C. Birch *et al.*, 1977 Genetic analysis of larval feeding behaviour in Drosophila melanogaster: II. Growth relations and competition between selected lines. Genet. Res. 30: 149.

Burns, J. G., N. Svetec, L. Rowe, F. Mery, M. J. Dolan *et al.*, 2012 Gene-environment interplay in Drosophila melanogaster: chronic food deprivation in early life affects adult exploratory and fitness traits. Proc. Natl. Acad. Sci. USA 109: 17239–17244.

Chintapalli, V. R., J. Wang, and J. A. Dow, 2007 Using FlyAtlas to identify better Drosophila melanogaster models of human disease. Nat. Genet. 39: 715–720.

de Belle, J. S., A. J. Hilliker, and M. B. Sokolowski, 1989 Genetic localization of foraging (for): a major gene for larval behavior in *Drosophila melanogaster*. Genetics 123: 157–63.

de Belle, J. S., M. B. Sokolowski, and A. J. Hilliker, 1993 Genetic analysis of the foraging microregion of Drosophila melanogaster. Genome 36: 94–101.

Demir, E., and B. J. Dickson, 2005 fruitless splicing specifies male courtship behavior in Drosophila. Cell 121: 785–794.

Edgar, B. A., 2006 How flies get their size: genetics meets physiology. Nat. Rev. Genet. 7: 907–916.

Fitzpatrick, M. J., and M. B. Sokolowski, 2004 In search of food: exploring the evolutionary link between cGMP-dependent protein kinase (PKG) and behaviour. Integr. Comp. Biol. 44: 28–36.

Friedrich, J., S. Sorge, F. Bujupi, M. P. Eichenlaub, N. G. Schulz *et al.*, 2016 Hox function is required for the development and maintenance of the Drosophila feeding motor unit. Cell Rep. 14: 850–860.

Gong, W. J., and K. G. Golic, 2003 Ends-out, or replacement, gene targeting in Drosophila. Proc. Natl. Acad. Sci. USA 100: 2556–2561.

Gong, W. J., and K. G. Golic, 2004 Genomic deletions of the Drosophila melanogaster Hsp70 genes. Genetics 168: 1467–1476.

Graveley, B. R., A. N. Brooks, J. W. Carlson, M. O. Duff, J. M. Landolin *et al.*, 2011 The developmental transcriptome of Drosophila melanogaster. Nature 471: 473–479.

Green, R. B., V. Hatini, K. A. Johansen, X.-J. Liu, and J. A. Lengyel, 2002 Drumstick is a zinc finger protein that antagonizes Lines to control patterning and morphogenesis of the Drosophila hindgut. Development 129: 3645–3656.

Groth, A. C., M. Fish, R. Nusse, and M. P. Calos, 2004 Construction of transgenic Drosophila by using the site-specific integrase from phage phiC31. Genetics 166: 1775–1782.

Holm, S. 1979 A simple sequentially rejective multiple test procedure. Scand. J. Stat. 6: 65–70.

Hoskins, R. A., J. M. Landolin, J. B. Brown, J. E. Sandler, H. Takahashi *et al.*, 2011 Genome-wide analysis of promoter architecture in Drosophila melanogaster. Genome Res. 21: 182–192.

Joshi, A., and L. D. Mueller, 1988 Evolution of higher feeding rate in Drosophila due to density-dependent natural selection. Evolution 42: 1090.

Kalderon, D., and M. Rubin, 1989 cGMP-dependent protein kinase genes in Drosophila. J. Biol. Chem. 264: 10738–10748.

Kanao, T., T. Sawada, S.-A. Davies, H. Ichinose, K. Hasegawa *et al.*, 2012 The nitric oxide-cyclic GMP pathway regulates FoxO and alters dopaminergic neuron survival in Drosophila. PLoS One 7: e30958.

Kaun, K. R., C. A. L. Riedl, M. Chakaborty-Chatterjee, A. T. Belay, S. J. Douglas *et al.*, 2007 Natural variation in food acquisition mediated via a Drosophila cGMP-dependent protein kinase. J. Exp. Biol. 210: 3547–3558.

Kaun, K. R., M. Chakaborty-Chatterjee, and M. B. Sokolowski, 2008 Natural variation in plasticity of glucose homeostasis and food intake. J. Exp. Biol. 211: 3160–3166.

Kearse, M., R. Moir, A. Wilson, S. Stones-Havas, M. Cheung *et al.*, 2012 Geneious basic: an integrated and extendable desktop software platform for the organization and analysis of sequence data. Bioinformatics 28: 1647–1649.

Kent, C. F., T. Daskalchuk, L. Cook, M. B. Sokolowski, and R. J. Greenspan, 2009 The Drosophila foraging gene mediates adult plasticity and gene-environment interactions in behaviour, metabolites, and gene expression in response to food deprivation. PLoS Genet. 5: e1000609.

Leopold, P., and N. Perrimon, 2007 Drosophila and the genetics of the internal milieu. Nature 450: 186–188.

Ling, D., and P. M. Salvaterra, 2011 Robust RT-qPCR data normalization: Validation and selection of internal reference genes during post-experimental data analysis. PLoS One 6: e17762.

Manning, G., G. D. Plowman, T. Hunter, and S. Sudarsanam, 2002 Evolution of protein kinase signaling from yeast to man. Trends Biochem. Sci. 27: 514–520.

Mery, F., A. T. Belay, A. K.-C. So, M. B. Sokolowski, and T. J. Kawecki, 2007 Natural polymorphism affecting learning and memory in Drosophila. Proc. Natl. Acad. Sci. USA 104: 13051–13055.

Michelson, A. M., and S. H. Orkin, 1982 Characterization of the homopolymer tailing reaction catalyzed by terminal deoxynucleotidyl transferase. Implications for the cloning of cDNA. J. Biol. Chem. 257: 14773–14782.

Miyashita, K., H. Itoh, H. Tsujimoto, N. Tamura, Y. Fukunaga *et al.*, 2009 Natriuretic peptides/cGMP/cGMP-dependent protein kinase cascades promote muscle mitochondrial biogenesis and prevent obesity. Diabetes 58: 2880–2892.

Ørstavik, S., V. Natarajan, K. Taskén, T. Jahnsen, and M. Sandberg, 1997 Characterization of the human gene encoding the type I alpha and type I beta cGMP-dependent protein kinase (PRKG1). Genomics 42: 311–318.

Osborne, K. A., A. Robichon, E. Burgess, S. Butland, R. A. Shaw *et al.*, 1997 Natural behavior polymorphism due to a cGMP-dependent protein kinase of Drosophila. Science 277: 834–836.

Parks, A. L., K. R. Cook, M. Belvin, N. A. Dompe, R. Fawcett *et al.*, 2004 Systematic generation of high-resolution deletion coverage of the Drosophila melanogaster genome. Nat. Genet. 36: 288–292.

Pearce, L. R., D. Komander, and D. R. Alessi, 2010 The nuts and bolts of AGC protein kinases. Nat. Rev. Mol. Cell Biol. 11: 9–22.

Peng, Q., Y. Wang, M. Li, D. Yuan, M. Xu *et al.*, 2016 cGMP-dependent protein kinase encoded by foraging regulates motor axon guidance in Drosophila by suppressing lola function. J. Neurosci. 36: 4635–4646.

Pfeifer, A., P. Klatt, S. Massberg, L. Ny, M. Sausbier *et al.*, 1998 Defective smooth muscle regulation in cGMP kinase I-deficient mice. EMBO J. 17: 3045–3051.

Ponton, F., M. P. Chapuis, M. Pernice, G. A. Sword, and S. J. Simpson, 2011 Evaluation of potential reference genes for reverse

transcription-qPCR studies of physiological responses in Drosophila melanogaster. J. Insect Physiol. 57: 840–850.

R Core Team 2016   R: A language and environment for statistical computing. R Foundation for Statistical Computing, Vienna, Austria. Available at: https://www.R-project.org/.

Raizen, D. M., K. M. Cullison, A. I. Pack, and M. V. Sundaram, 2006   A novel gain-of-function mutant of the cyclic GMP-dependent protein kinase egl-4 affects multiple physiological processes in Caenorhabditis elegans. Genetics 173: 177–187.

Ryder, E., F. Blows, M. Ashburner, R. Bautista-Llacer, D. Coulson et al., 2004   The DrosDel collection: a set of P-element insertions for generating custom chromosomal aberrations in Drosophila melanogaster. Genetics 167: 797–813.

Sambrook, J., and D. W. Russell, 2001   Molecular Cloning: A Laboratory Manual, Ed. 3. Cold Spring Harbor Laboratory Press, Cold Spring Harbor, New York.

Schindelin, J., I. Arganda-Carreras, E. Frise, V. Kaynig, M. Longair et al., 2012   Fiji: an open-source platform for biological-image analysis. Nat. Methods 9: 676–682.

Schoofs, A., S. Hückesfeld, P. Schlegel, A. Miroschnikow, M. Peters et al., 2014   Selection of motor programs for suppressing food intake and inducing locomotion in the Drosophila brain. PLoS Biol. 12: e1001893.

Sewell, D., B. Burnet, and K. Connolly, 1974   Genetic analysis of larval feeding behaviour in Drosophila melanogaster. Genet. Res. 24: 163.

Siegal, M. L., and D. L. Hartl, 1996   Transgene coplacement and high efficiency site-specific recombination with the Cre/loxP system in Drosophila. Genetics 144: 715–726.

Sokolowski, M. B., 1980   Foraging strategies of Drosophila melanogaster: a chromosomal analysis. Behav. Genet. 10: 291–302.

Sokolowski, M. B., 2001   Drosophila: genetics meets behaviour. Nat. Rev. Genet. 2: 879–890.

Sokolowski, M. B., 2010   Social interactions in "simple" model systems. Neuron 65: 780–794.

Sokolowski, M. B., H. S. Pereira, and K. Hughes, 1997   Evolution of foraging behavior in Drosophila by density-dependent selection. Proc. Natl. Acad. Sci. USA 94: 7373–7377.

Stansberry, J., E. J. Baude, M. K. Taylor, P. J. Chen, S. W. Jin et al., 2001   A cGMP-dependent protein kinase is implicated in wild-type motility in C. elegans. J. Neurochem. 76: 1177–1187.

Stapleton, M., G. Liao, P. Brokstein, L. Hong, P. Carninci et al., 2002   The Drosophila gene collection: identification of putative full-length cDNAs for 70% of D. melanogaster genes. Genome Res. 12: 1294–1300.

Taylor, S., M. Wakem, G. Dijkman, M. Alsarraj, and M. Nguyen, 2010   A practical approach to RT-qPCR-publishing data that conform to the MIQE guidelines. Methods 50: S1–S5.

Thorpe, H. M., and M. C. Smith, 1998   In vitro site-specific integration of bacteriophage DNA catalyzed by a recombinase of the resolvase/invertase family. Proc. Natl. Acad. Sci. USA 95: 5505–5510.

Venken, K. J. T., Y. He, R. A. Hoskins, and H. J. Bellen, 2006   P [acman]: a BAC transgenic platform for targeted insertion of large DNA fragments in D. melanogaster. Science 314: 1747–1751.

Warming, S., N. Costantino, D. L. Court, N. A. Jenkins, and N. G. Copeland, 2005   Simple and highly efficient BAC recombineering using galK selection. Nucleic Acids Res. 33: e36.

Weber, S., D. Bernhard, R. Lukowski, P. Weinmeister, R. Wörner et al., 2007   Rescue of cGMP kinase I knockout mice by smooth muscle specific expression of either isozyme. Circ. Res. 101: 1096–1103.

Communicating editor: M. F. Wolfner